Thermochimica Acta, 200 (1992) 151–167
Elsevier Science Publishers B.V., Amsterdam

Differential thermal analysis, thermogravimetry and in-source pyrolysis-mass spectrometry studies on the formation of soil organic matter

P. Leinweber [a] and H.-R. Schulten [b]

[a] *Institute for Structural Analysis and Planning in Areas of Intense Agriculture, University of Osnabrück, Driverstrasse 22, P.O. Box 1553, 2848 Vechta (Germany)*
[b] *Department of Trace Analysis, Fachhochschule Fresenius, Dambachtal 20, 6200 Wiesbaden (Germany)*

(Received 3 March 1992)

Abstract

Differential thermal analysis (DTA) thermogravimetry (TG) and pyrolysis-field ionization mass spectrometry (Py–FIMS) were compared in studies of soil organic matter (SOM) in particle-size fractions in different years of a long-term soil formation experiment with loamy marl. The DTA curves and TG weight losses indicated the presence of different amounts of SOM, quartz and carbonates in the various size fractions and experimental years. The soil development from the 2nd to the 34th experimental year was characterized by the enrichment of SOM in the size fractions investigated, which also resulted in an accelerated weathering of carbonates.

The comparison between DTA curves, TG weight losses and Py–FIMS thermograms and weight losses, respectively, showed a shift of the maximum of thermal decomposition of SOM to higher temperatures in Py–FIMS. This was explained by the higher heating rate (0.5 K s^{-1}) and the particularly large sample amounts (5 mg) used in the mass spectrometric studies of particle-size fractions of whole soils with organic carbon (C_{org}) concentrations between 0.2 and 1.9%. However, the onset of thermal evolution was in good agreement with DTA and TG data. Similar results were also obtained in the thermal behaviour of particle-size fractions and changes during soil development.

By Py–FIMS, complementary information was obtained about the molecular chemical composition of SOM in the fractions by the evaluation of summed and averaged mass spectra and by the assignment of signals to the principal classes of chemical compounds. The abundances of phenols and lignin monomers and N-compounds decreased with increasing particle size; the reverse was true for lignin dimers and fatty acids. The latter two compound classes were also enriched in the samples from the 34th experimental year owing to SOM maturation. A unique feature of Py–FIMS as a novel method of whole soil analysis was its high analytical resolution which allowed monitoring of the thermal evolution of selected classes of compounds on a molecular chemical basis. This was demonstrated for the first time for phenols and lignin monomers, lignin dimers and alkylaromatics which are

Correspondence to: H.-R. Schulten, Department of Trace Analysis, Fachhochschule Fresenius, Dambachtal 20, 6200 Wiesbaden, Germany.

important soil constituents for SOM formation as well as for agricultural and environmental problems.

INTRODUCTION

Thermal degradation techniques, such as differential thermal analysis (DTA), thermogravimetry (TG) and differential thermogravimetry (DTG), have been used for many years in studies of soil organic matter (SOM) [1]. Information on the structure of SOM was obtained by graded pyrolysis, followed by wet chemical and spectroscopic analyses of samples withdrawn at regular temperature intervals [2]. Based on these investigations, the results of DTA, TG and DTG from some recent studies were used to explain SOM-determined soil properties, such as degree of mineralization in humus horizons [3], mechanical stability of sandy soils [4] and SOM changes due to different long-term soil management systems [5]. Therefore it appeared appropriate to search for an improved interpretation basis of DTA, TG and DTG data. One approach included the combination of either temperature-programmed, in-source or Curie-point pyrolysis with mass spectrometry for the analyses of SOM volatiles and pyrolysis products, sometimes after gas chromatographic separation [6]. In particular, pyrolysis–field ionization mass spectrometry (Py–FIMS), was used recently for extensive studies of extracted humic substances [7], soil particle-size fractions [8] and whole soil samples of different origin and management systems [9]. Moreover, the explanation for various chemical [10] and physical soil properties has been given [11,12]. In a methodological comparison of DTA, TG and Py–FIMS, similarities were found in the shapes of DTA curves and Py–FIMS thermograms as well as significant correlations between the weight losses determined directly by TG and those calculated from molecular masses and ion intensities registered by Py–FIMS [13].

The objective of the present study was to improve the molecular chemical knowledge for the interpretation of DTA and TG data. This was connected with studies of the initial formation of SOM from grass residues in particle-size fractions which were originally largely free of humus. Thus, samples were analysed from the Rostock long-term pot experiment on humus formation and soil development (Hu3) which was started with loamy marl [14]. The following points were of particular interest in this study:

(i) to follow the development of organo–mineral particle-size fractions during a 34 year period of mineral weathering, SOM enrichment and initial soil formation in loamy marl by DTA and TG analyses;

(ii) to compare DTA, TG results with Py–FI thermograms and calculated weight losses in order to evaluate the agreement in basic thermal properties;

(iii) to demonstrate the potential of Py–FIMS to produce information on the molecular chemical composition of SOM in the soil fractions and on

the temperature dependence for the evolution of selected chemical classes of SOM constituents.

EXPERIMENTAL

Long-term experiment, soil samples and particle-size fractions

The Rostock long-term pot experiment on humus formation and soil development (Hu3) was started in 1954, using practically humus-free, pleistocene loamy marl (about 20% clay, 42% silt, 38% sand and 33% $CaCO_3$) as parent material. This substrate was continuously grown with grass. A detailed description of the experimental set-up, and principal results concerning the development of SOM contents [14,15] and of humus quality have been reported [16]. Soil samples from the mineral fertilization variant ($KNO_3 + KH_2PO_4$), collected in the 2nd, 7th, 13th, 19th and 34th experimental year, were separated into organo-mineral particle-size fractions: clay (less than 2 μm), fine silt (2–6.3 μm), medium silt (6.3–20 μm), coarse silt (20–63 μm). The method of ultrasonic disaggregation and particle-size fractionation was similar to that described in ref. 17. Selected characteristics of the samples are listed in Table 1.

Differential thermal analysis (DTA) and thermogravimetry (TG)

For DTA and TG analysis, about 300 mg of sample were heated continuously from 20 to 1000°C at a heating rate of 0.17 K s^{-1} in an atmosphere of air. The DTA, TG and DTG curves were recorded simultaneously using a Q 1500-D derivatograph (MOM, Budapest, Hungary). Weight losses per 50 K and per 100 K were calculated from the TG curves.

Pyrolysis-field ionization mass spectrometry (Py–FIMS)

For temperature-resolved Py–FIMS about 5 mg of the samples (clay, fine silt and medium silt, 13th and 34th experimental years) were thermally degraded in the ion source of a Finnigan MAT 731 mass spectrometer. The heatable/coolable direct introduction system with electronic temperature programming (IGT Instrumente- and Geräte-Technik GmbH, 5203 Much, Germany), adjusted at the +8 kV potential of the ion source, was used. All samples were heated in high vacuum from 50 to 700°C at a heating rate of approximately 0.5 K s^{-1} [18]. About 60 magnetic scans were recorded for the mass range 16–1000 Da. Three to four replicates were performed for each sample. The weight losses during pyrolysis were computed by multiplying the intensities of the registered ions with their molecular masses. The total ion intensities (TII) of the single spectra were plotted versus pyrolysis temperature after they were averaged for the replicate runs,

resulting in Py–FIMS thermograms. The single spectra were integrated by the Finnigan MAT SS 200 data system, resulting in summed spectra. From these summed spectra, weight- and number-averaged molecular weights were calculated according to ref. 19. Further, the data of the replicate spectra were averaged to one survey spectrum for each sample. From the mass lists of these survey spectra, the relative abundances of various classes of chemical compounds were calculated using characteristic mass signals [20,21]. This was also performed for 60 single spectra of the medium-silt samples from the 13th and the 34th experimental years. A detailed description of the Py–FIMS methodology can be found in ref. 22.

RESULTS AND DISCUSSION

Differential thermal analysis and thermogravimetry

The DTA curves of the organo–mineral clay and fine-silt fractions are displayed in Fig. 1, and of the medium- and coarse-silt fractions in Fig. 2. These curves exhibit exothermic and endothermic reactions in all samples. The exotherms between 200 and 600°C point to the oxidation of SOM during DTA. This is always followed by a strong endothermic effect with a maximum between 850 and 925°C, indicative of the thermal decomposition of carbonate minerals (calcite, dolomite). Differences between the size fractions are observed in the intensities of these effects in so far as the SOM exotherms decrease in the order clay, medium silt > fine silt > coarse silt. Further, the order fine silt > medium silt > clay > coarse silt is obtained for the intensities of the carbonate endotherms. In addition, the endothermic quartz conversion is detected only in the medium- and coarse-silt fractions in Fig. 2. Clear differences are also visible when comparing the curves of each corresponding size fraction for the different experimental years. The SOM exotherms around 300–400°C and 500°C increase with time. The reverse is true for the endothermic decarbonization. Furthermore, the endothermic dehydratation (100–200°C) is more strongly developed in the samples of the later experimental years. The sharp exotherm around 950°C in the clay sample from the 34th year may be due to illites [23], pedogene iron oxides or gehlenite ($Ca_2Al_2SiO_7$), formed during heating [24].

The TG weight losses per 100 K, corresponding to the DTA curves in Figs. 1 and 2, were calculated from the TG curves. Since the organic matter decomposition is largely completed at 600°C (Figs. 1 and 2) only the weight losses up to this temperature are shown in Table 2. The highest weight losses per 100 K are detected in the early experimental years at above 400–600°C (clay and fine silt, 2nd to 13th year; medium and coarse silt, 2nd to 7th year). During soil development and SOM formation the highest values of TG weight losses appear to shift towards lower temperatures (see

TABLE 1

Selected characteristics of the samples

Size fraction	Sampling year	Percentage soil d.w. [a]	$CaCO_3$ (%) [b]	C_{org} ratio	C/N ratio	SOM proportions [c]	
						C_{org} (%)	N_t (%)
Clay	2	18.7	55.8	0.49	8.2	36.4	17.1
	7	18.3	48.3	1.18	8.4	n.d. [d]	59.8
	13	21.3	48:0	1.74	6.7	52.4	67.3
	19	18.5	47.2	2.05	8.2	51.4	60.2
	34	18.9	43.8	3.04	7.4	49.8	58.0
Fine silt	2	12.4	47.4	0.75	6.8	31.3	53.4
	7	12.3	57.2	0.56	14.0	n.d. [d]	12.4
	13	10.6	59.7	0.61	8.7	11.7	8.8
	19	13.3	58.8	0.80	10.0	18.3	13.5
	34	12.3	52.5	1.66	11.1	21.0	14.5
Medium silt	2	10.8	36.0	0.46	11.5	13.6	14.8
	7	9.6	21.8	n.d. [d]	n.d. [d]	n.d. [d]	10.3
	13	11.0	33.8	1.11	18.5	13.5	8.7
	19	10.8	32.8	1.42	12.9	16.2	15.4
	34	10.8	30.2	1.94	12.9	14.7	12.7
Coarse silt	2	8.2	22.4	0.21	10.5	4.0	7.5
	7	10.9	21.9	n.d. [d]	n.d. [d]	n.d. [d]	7.7
	13	9.6	23.8	0.44	11.0	4.1	4.6
	19	10.2	22.8	0.43	14.3	4.1	3.6
	34	11.1	20.0	0.69	11.5	4.7	5.3

[a] Proportions of fraction dry matter in the whole soil samples.

[b] Determined by dissolution in HCl, followed by volumetric CO_2 analysis.

[c] Distribution of whole soil organic matter on the size fractions, (organic carbon and total nitrogen, normalized to 100%).

[d] Not determined.

Table 2). A refined evaluation of the weight losses in 50 K increments indicates that a second maximum developed with time in the range 500–550°C. The DTG curves show distinct peaks only at 300 (SOM oxidation) and 900°C (decomposition of carbonate minerals) (not shown).

These results are interpreted as follows: the thermal reactions point to the presence of absorbed water, organic matter, quartz and carbonates (sequence according to increasing temperatures of characteristic reactions). The exothermic peak in the DTA curves of clay, for the 34th year, is assigned to pedogene iron oxides and/or to illite, rather than to gehlenite, since it appears to be a product of mineral weathering and soil formation. The increases in the SOM exotherms toward finer particle-sizes, and with time, indicate characteristic enrichments in newly formed SOM. This is supported by the increased TG weight losses with time (Table 2) and by strong linear correlations between the C_{org} as well as total N concentra-

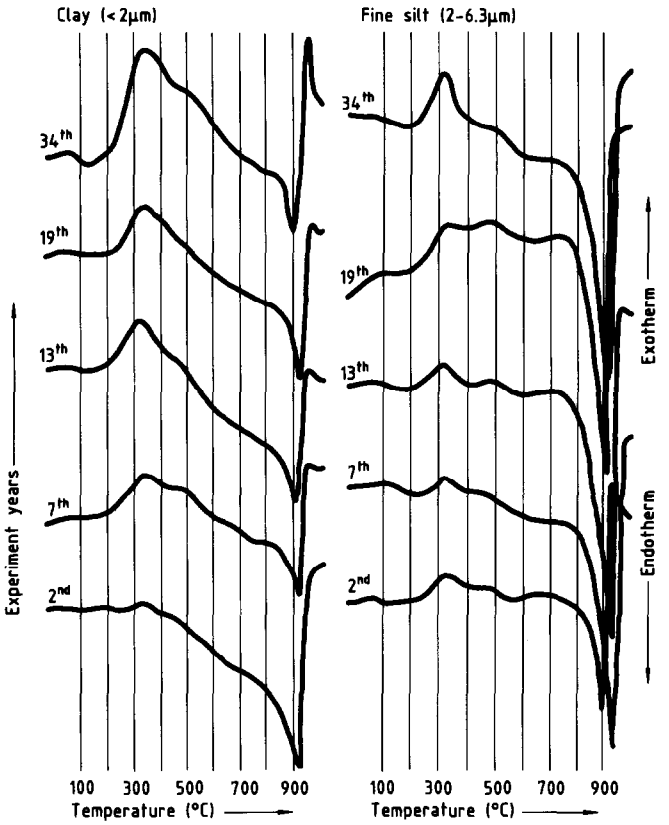

Fig. 1. DTA curves of clay and fine-silt fractions of different years of the long-term experiment Hu3.

tions and the TG weight losses between 100 and 600°C (correlation coefficient $r = 0.92***$ and $r = 0.97***$ respectively, error probability $p = 0.001$). The shifts of the maximal TG weight losses to lower temperatures indicate that the majority of organic substances accumulated in fractions in the later experimental period (after about 7–13 years) is of a lower thermal stability. However, in addition to this dominating process, SOM or organo–mineral complexes with high thermal stability were also formed during the experiment, as the exotherms at 500–600°C in Fig. 1 indicate. This appears to be more favoured in the medium-silt fraction and agrees with DTA and TG studies of organo–mineral clay fractions and two density fractions of silt-size particles from a wide range of Japanese soils [25]. In the cited paper it was reported that the dominant exothermic reaction during DTA of clay occurred at 290–310°C and was assigned to the liberation of aliphatics and to decarboxylation. In contrast, specific light ($\rho < 1.7$ g cm^{-3}) and dark coloured silt-size particles showed only a

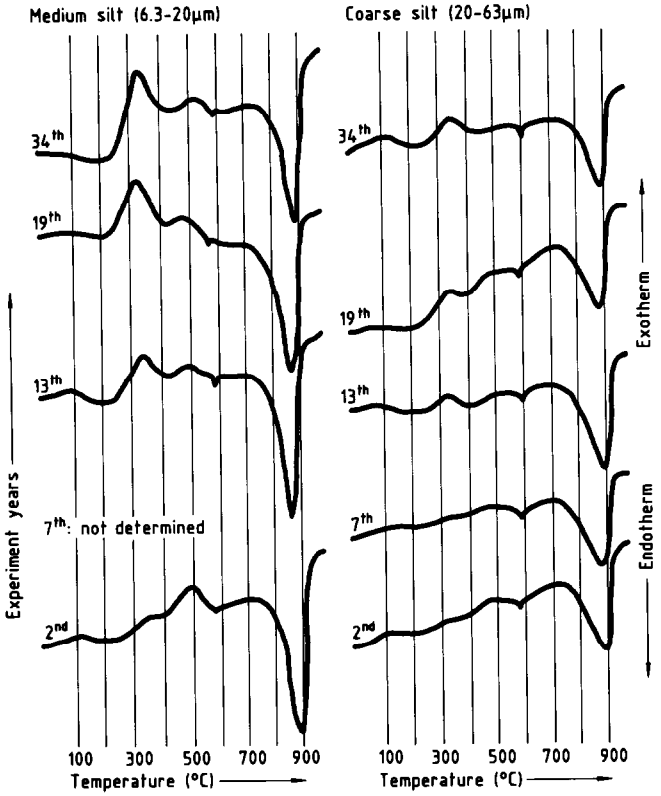

Fig. 2. DTA curves of medium-silt and coarse-silt fractions of different years of the long-term experiment Hu3.

high temperature exothermic reaction at 400–450°C, which was attributed to the decomposition of aromatics. For heavier ($\rho = 1.7$–2.0 g cm^{-3}) and brown coloured silt-size particles exotherms at low and high temperatures were observed [25]. The comparison of the DTA curves in Figs. 1 and 2 with analogous curves from the "Ewiger Roggenbau" experiment ("Eternal rye cultivation" at Halle, Germany) [13] shows far more intense effects in the higher temperature range for the latter. This indicates a higher thermal stability of SOM due to stronger bonding and cross-linking. Clearly, this can be interpreted as a result of more than 10000 years of soil formation and SOM maturation.

The weathering of the carbonate minerals is related to the SOM enrichment. This is confirmed by the fact that the carbonate contents calculated from the TG curves, in agreement with calcite contents obtained by X-ray diffraction and by wet chemical analyses, were negatively correlated to the C_{org} and N concentrations [26].

TABLE 2

Thermogravimetry: weight losses per 100 K in size fractions of different years of the experiment Hu3 (percentage of sample weight; the highest values for each sampling year are printed in italics)

Size fraction	Sampling year	Temperature (°C)					
		20–100	100–200	200–300	300–400	400–500	500–600
Clay	2	0.2	0.1	0.3	0.4	0.4	*1.0*
	7	0.6	0.7	0.8	1.0	0.9	*1.5*
	13	0.9	0.8	1.3	1.3	1.3	*1.6*
	19	0.7	0.7	1.3	*1.5*	1.2	1.4
	34	0.7	1.4	2.0	*2.3*	1.9	2.2
Fine silt	2	0.6	0.7	0.4	0.6	0.9	*1.6*
	7	0.0	0.0	0.3	0.5	*0.6*	*0.6*
	13	0.0	0.1	0.4	0.6	0.4	0.7
	19	0.0	0.2	0.5	*0.6*	0.3	*0.6*
	34	0.0	0.3	0.9	*1.3*	0.5	0.8
Medium silt	2	0.0	0.0	0.0	0.2	0.3	*0.4*
	7	Not determined					
	13	0.0	0.1	0.5	*0.8*	0.3	0.5
	19	0.0	0.2	0.9	*1.1*	0.4	0.6
	34	0.2	0.3	1.1	*1.6*	0.6	0.6
Coarse silt	2	0.0	0.0	0.0	0.0	0.1	*0.2*
	7	Not determined					
	13	0.0	0.0	0.0	*0.4*	0.2	0.3
	19	0.0	0.0	0.1	*0.4*	0.1	*0.4*
	34	0.0	0.0	0.3	*0.6*	0.2	0.3

Comparison of Py–FIMS thermograms and weight losses to DTA curves and TG

Averaged Py–FIMS thermograms and the corresponding weight loss curves are shown in Fig. 3. The peaks in the Py–FIMS thermograms are generally observed at temperatures 20–100 K higher than at those in the equivalent DTA curves in the Figs. 1 and 2. These shifts are more pronounced in fine silt and clay as well as in the 13th experimental year. This is partly explained by the different heating rates of 0.5 K s^{-1} in the Py–FIMS and of 0.17 K s^{-1} in DTA. For amphiphilic copolymers, it was found that the heating rates of DTA, TG and Py–FIMS influenced the pathway and the resolution of thermal degradation into distinct reaction steps [27,28]. For two organo–mineral soil clay samples, the adaption of the heating rates to 0.2 K s^{-1} shifted the maxima of TII in the Py–FIMS toward lower temperatures (−20 K), thereby obtaining a better agreement with the shapes of the DTA curves [13]. Nevertheless, the Py–FIMS thermograms for the fine- and medium-silt fractions are similar to the

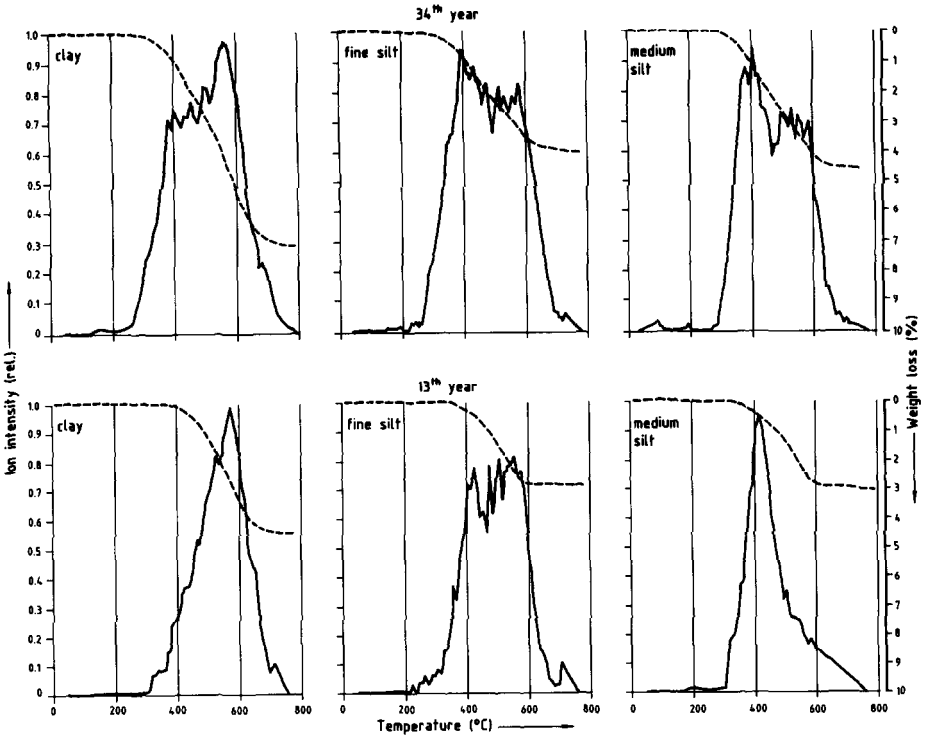

Fig. 3. Pyrolysis–field ionization mass spectrometry: thermograms (abscissa: left-hand side, total ion intensity relative to the maximal value; ordinate: pyrolysis temperature) and calculated weight losses (%) (on the right-hand side) of particle-size fractions for the 13th and 34th year of the Hu3 experiment.

corresponding DTA curves, which are probably less influenced by thermal reactions of the layer silicates, such as dehydratation and dehydroxylation, than the DTA of clay fractions. Furthermore, the onset temperatures of thermal decomposition appeared closely correlated in DTA and Py–FIMS (see Figs. 1 and 2, and compare with Fig. 3). This indicates that, in addition to the discussed influence of heating rates, the large sample amounts of 5 mg in Py–FIMS also caused a shift of the maxima of TII towards higher temperatures.

The weight loss curves in Fig. 3 show that the decomposition of SOM becomes intense at 300°C and is largely completed at approximately 600°C (silt) to 650°C (clay). At that temperature, between 2% and 7% of the original substance is thermally decomposed. The weight losses are highest in the clay fractions and decrease with particle size. Larger values are always found in the samples from the 34th experimental year (see Fig. 3). This is similarly observed by TG (Table 2); accordingly a close linear correlation exists between the weight losses calculated from the Py–FIMS data and those measured directly by TG (temperature range: 50–700°C,

TABLE 3

Weight averaged ($\overline{M}_w$) and number-averaged molecular weights ($\overline{M}_n$) of grass residues, whole soil samples and organo–mineral particle-size fractions from different years of the experiment Hu3

Sample	$\overline{M}_w$ (Da)		$\overline{M}_n$ (Da)		$\overline{M}_w / \overline{M}_n$	
	13	34	13	34	13	34
Grass residues	391.0 [a]		303.6		1.3	
Clay	203.4 ***[b] *	221.2 ***	165.0	175.9 *	1.2	1.3
Fine silt	241.4 *	263.7 ***	204.4	215.8 ***	1.2	1.2
Medium silt	281.2 *	321.4	227.0	281.6	1.2	1.1
Whole soil	230.5	207.6	187.3	167.4	1.2	1.2

[a] Means of each of two samples from stems and leaves and from roots.
[b] Significance level of differences: *, $p = 0.05$; **, $p = 0.01$; ***, $p = 0.001$.

$r = 0.955$**, $n = 6$). This is also true when comparing the weight losses for 50 K increments. In that case, the correlation coefficients decrease gradually from $r = 0.477$** ($n = 42$; 350–650°C) when the weight losses at higher and at lower temperatures are introduced stepwise into the regression analysis. This means that the two methods of determining weight losses during heating of organo–mineral fractions agree sufficiently in the temperature range which is particularly characterized by the thermal decomposition of SOM. In summarizing this methodological comparison it is confirmed that DTA, TG and Py–FIMS result in data with similar trends in SOM differences between size fractions and experimental years as well as fertilization variants as reported in ref. 13.

Qualitative investigation of thermal degradation products by Py–FIMS

Weight-averaged ($\overline{M}_w$) and number-averaged molecular weights ($\overline{M}_n$) of grass residues, size fractions and whole soil samples of the 13th and 34th experimental years are shown in Table 3. The grass residues have the largest molecular weight averages. In general, $\overline{M}_w$ and $\overline{M}_n$ increase with particle size, and in the 34th year. These data indicate a stronger influence of less-decomposed organic matter from grass on the mass spectra of coarser fractions and later experiment periods. However, it is surprising that in the whole soil samples, reduced mean molecular weights are found in the 34th year.

The Py-FI mass spectra of the clay, fine silt and medium silt fractions isolated from soil samples of the 13th experimental year are shown in Fig. 4(a)–(c). The presence of aromatic compounds such as phenols and lignin monomers is indicated by m/z 94, 108, 110, 120, 122, 124, 138, 150, 152,

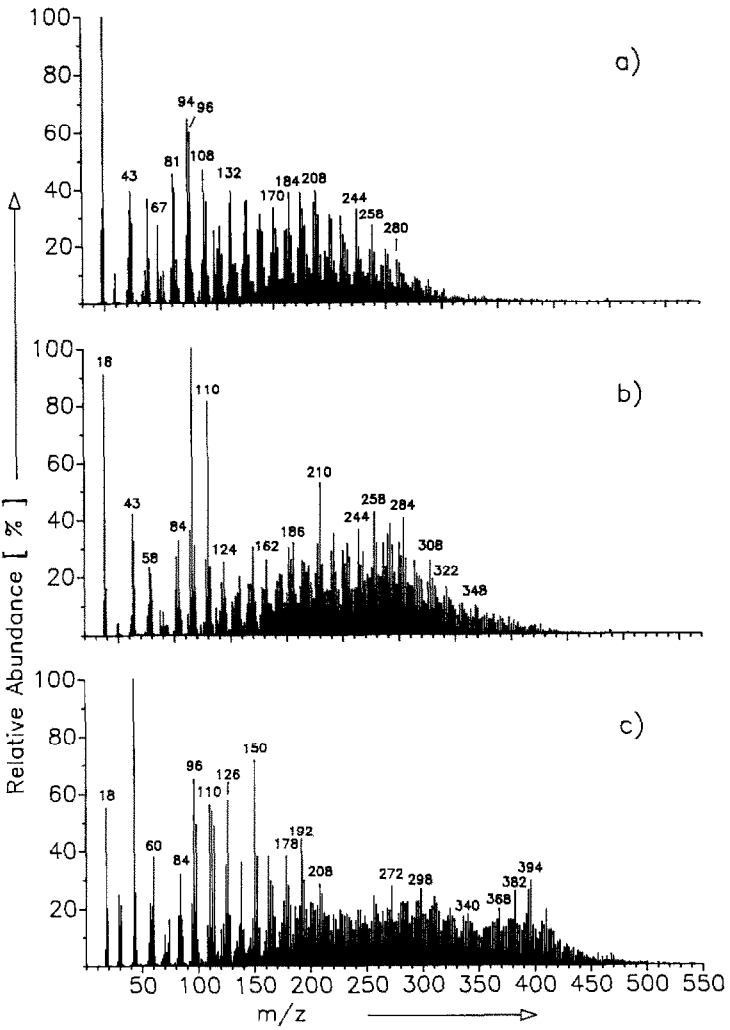

Fig. 4. Integrated and averaged Py–FI survey mass spectra of (a) clay, (b) fine silt, and (c) medium silt of the 13th year of the Hu3 experiment.

164, 166, 168, 178, 180, 182, 186, 192, 194, 196, 208, 210 and 212. The comparison of the spectra shows clear differences in the relative abundances of some of these signals. The same is true for lignin dimers (*m/z* 246, 260, 270, 272, 274, 284, 286, 296, 298, 300, 302, 310, 312, 314, 316, 326, 328, 330, 332, 340, 342, 356, 358 and 418), which are particularly intense in the spectrum of fine silt (Fig. 4(b)). Alkylaromatics were indicated by *m/z* 92, 106, 120, 134, 138, 148, 162, 176, 190, 204, 218, 232, 246, 260, 274, 288, 302, 316, 330, 344, 358, 372, 386 (alkylbenzenes), *m/z* 142, 156, 170, 184, 198 (alkylnaphthalenes) and *m/z* 192, 206, 220, 234 (alkylphenanthrenes). Within the group of aliphatic compounds signals indicative of monosaccha-

rides and polysaccharides dominate in the lower mass range: *m/z* 58, 60, 82, 84, 86, 96, 98, 110, 112, 114, 126, 128, 132, 144, 162. Some of these signals are very intense in distinct fractions such as *m/z* 82, 144 and 162 in clay (Fig. 4(a)) and *m/z* 84, 98, 112, 126 and 162 in fine and medium silt (Fig. 4(b) and (c)). Homologous series of signals can be assigned to fatty acids, starting at *m/z* 186 (C_{11}) to *m/z* 494 (C_{33}). For this sequence of signals, a clear trend of increasing intensities is observed with equivalent diameters, as shown by the high relative abundances of *m/z* 256, 270, 284 and 298 in fine silt, and *m/z* 228, 242, 256 and 368, 382, 396 and 410 in medium silt. In all size fractions, series of signals can be tentatively assigned to alkanes/alkenes. The following signals are particularly intense: *m/z* 156, 170, 184, 198) in the clay (C_{11-14}, possibly partly also originating from alkylnaphthalenes) and *m/z* 224, 226, 252, 254, 268, 280, 282, 294, 296, 308 and 322 in the fine silt (C_{17-24}), and *m/z* 266, 268, 280, 282, 294, 296, 308, 310, 322, 324, 336, 338, 350, 352, 364, 366, 378, 380, 392, 394, 406, 408, 420 and 422 (C_{19-30}) in the medium-silt sample. Some very intense signals in Fig. 4(a) (*m/z* 230, 244 and 258) may originate from a homologuous series of alkyl diesters. Nitrogen compounds (*m/z* 67, 79, 81, 95, 107, 117, 131, 145, 159 and 173), in particular heterocycles, appear especially enriched in the clay sample, and decrease with increasing particle size.

The Py–FI mass-spectra of the samples from the 34th experimental year are shown in Fig. 5(a)–(c). In general, the same mass-signals are observed, with the trend of a slight shift towards higher molecular masses. This is particularly clear in the spectrum of the medium-silt sample in Fig. 5(c). The most intense signals come from ions of higher molecular masses (*m/z* 200–450). This spectrum strongly resembles spectra of the grass residues [29], indicating the presence of relatively undecomposed organic matter in this fraction.

To focus on differences in the bulk chemical composition of the organic matter in the various size fractions as well as on its development during the experiment, the relative abundances of the principal classes of chemical compounds are listed in Table 4. Signal intensities indicative of phenols and lignin monomers decrease with increasing particle size, the reverse being true for lignin dimers. Monosaccharides and polysaccharides show some differences between size fractions but no uniform trend for the two experimental years. For fatty acids, considerable increases are found with the equivalent diameters of the fractions. The proportion of N compounds, in turn, falls from 14–12% in clay to 4–3% in medium silt. Within this group, heterocycles predominate, and they also show the strongest decreases towards the coarser size fractions. Differences between the sampling years are indicated by reduced relative abundances of phenols and lignin monomers in the 34th experimental year. In turn, lignin dimers and fatty acids appear enriched in all fractions, and in clay and fine-silt fractions, respectively. Monosaccharides and polysaccharides show en-

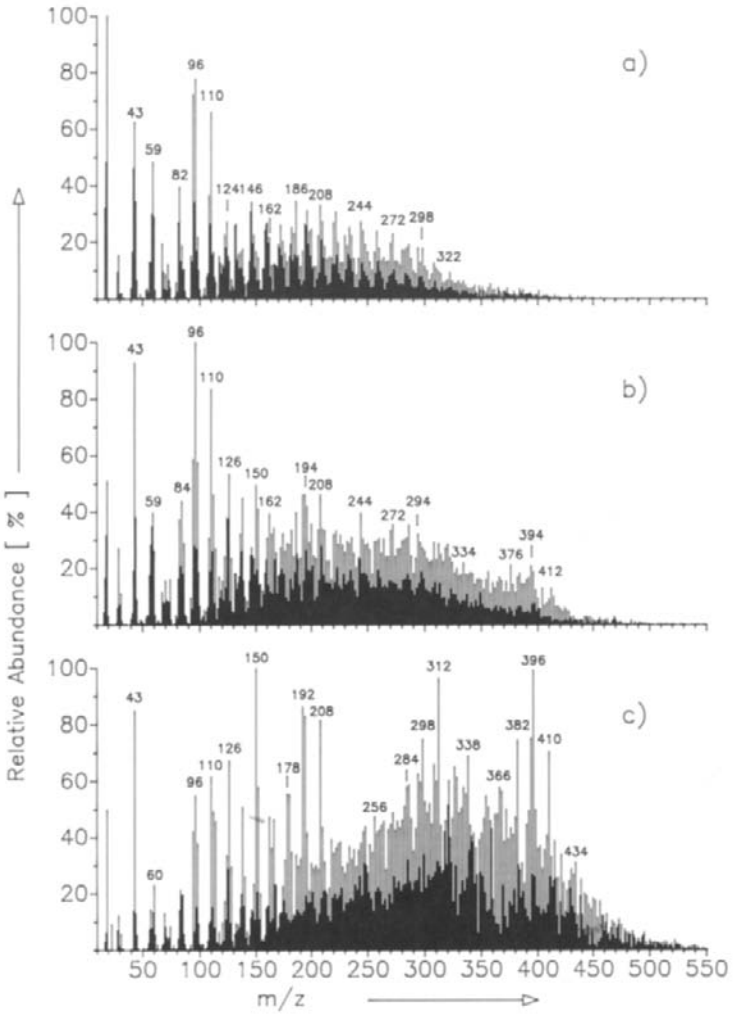

Fig. 5. Integrated and averaged Py–FI survey mass spectra of (a) clay, (b) fine silt, and (c) medium silt of the 34th year (cf. Fig. 4).

hanced values in the clay fraction and are reduced in the medium silt. The ion intensities for N compounds are relatively unchanged.

The mass spectral differences between the particle-size fractions are in very good agreement with the corresponding data obtained in Py–FIMS studies of equivalent size fractions from soils of the "Ewiger Roggenbau" field experiment [13]. As in that set of samples, a significant correlation is found between the N concentrations of organic matter and the summed ion intensities for N compounds ($r = 0.893$*). The comparison of the size fractions from the 13-year-old or 34-year-old Hu3 pot experiment with the equivalent fractions from the more than 10 000 years older soil of the

TABLE 4

Pyrolysis–field ionization mass spectrometry: relative abundances of selected classes of chemical compounds in different size fractions and years of the experiment Hu3 (units are percentages of total ion intensity)

Class of compound	Size fractions and experimental years					
	Clay		Fine silt		Medium silt	
	13	34	13	34	13	34
Aromatics						
Phenolics, lignin monomers	17.8	15.6	15.5	13.4	14.6	10.4
Lignin dimers	4.8	6.5	10.9	8.4	8.9	11.6
Aliphatics						
Monosaccharides and polysaccharides	8.6	9.8	10.2	9.5	11.2	4.5
Alkanes/alkenes	3.3	2.4	2.9	3.0	3.2	3.3
Fatty acids	1.8	2.4	4.4	4.0	5.7	8.0
N compounds						
Nitriles	0.9	0.9	0.6	0.8	0.4	0.3
Amino-N/amides	2.5	2.8	1.4	1.7	1.2	0.6
Heterocycles	10.2	8.2	3.9	4.5	2.5	1.8

"Ewiger Roggenbau" experiment indicates lower relative abundances of aromatic compounds, especially phenols and lignin monomers in the latter as well as a higher level of N compounds which originates especially from amino nitrogen and amides.

Recently, the distribution of selected classes of compounds has been reported for SOM formation in whole soil from this long-term experiment [29]. The thermal evolution of phenols and lignin monomers, lignin dimers and alkylaromatics is shown in Fig. 6 for the medium-silt fraction of the 13th and 34th experimental year. In the 13th year (Fig. 6(b)), the intensities of marker molecules for these compounds show an approximately gaussian distribution with maxima at 400–415°C. In the 34th year, however, a curve with two discrete peaks is obtained for lignin dimers and alkylaromatics (Fig. 6(b)). These curves demonstrate for the first time that an improved analytical resolution of the TII curves in Fig. 3 can be obtained by the monitoring of thermal evolution of selected compound classes. The second peaks at 510–530°C visualize that amounts of these substances have reached a higher thermal stability in the time period from the 13th to 34th experimental year. This thermal stabilization is interpreted as a result of three-dimensional cross-linking of these compounds during SOM maturation. This view is in agreement with the proposal that alkylaromatics are significant structural building blocks of humic substances which form a sponge-like network structure that can trap and bind carbohydrates, proteins, lipids, biocides as well as inorganics [30]. Furthermore, the macromolecular stabilization of alkylaromatics, indicated by the second peak in

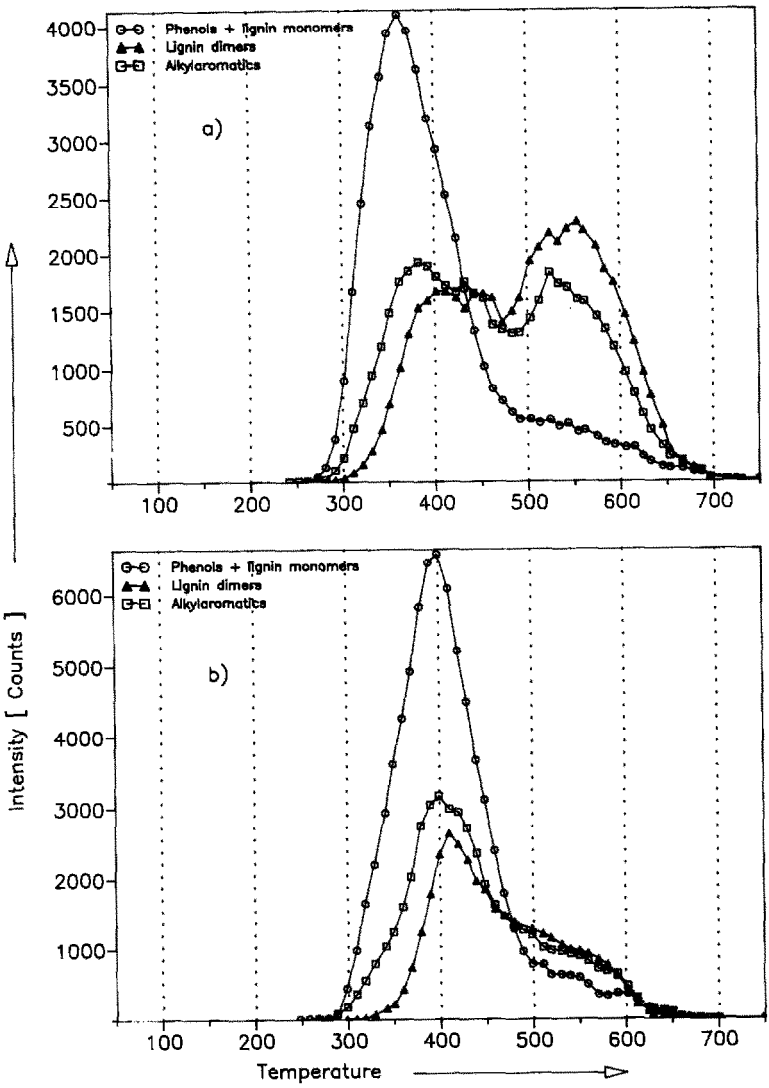

Fig. 6. Temperature profiles for the evolution of selected classes of compounds for (a) the 34th and (b) the 13th experimental year: ○, phenols and lignin monomers; ▲, lignin dimers; □, alkylaromatics.

Fig. 6(a) explains why these componds are considerably enriched with time in whole soil samples [29].

CONCLUSIONS

By DTA and TG, it is found that 34 years of development of organo–mineral size fractions is characterized by considerable enrichment in SOM. This results in enhanced weathering of carbonates from the original marl.

The shapes of the DTA curves and the TG weight losses confirm the results of the inorganic and organic carbon determinations, and give a first indication of qualitative differences between SOM in size fractions and experimental years.

By time/temperature-resolved Py–FIMS, relevant information is obtained on the molecular composition of the substances delivered during thermal breakdown of SOM. From the agreement of DTA curves and Py–FIMS thermograms, it is concluded that correlations exist between the amount of energy that is stored in chemical bonding and is converted into heat during DTA and the number of molecules that are associated in SOM as registered during Py–FIMS. The consideration of the corresponding molecular weights in Py–FIMS enables a calculation of weight losses. These results correlate significantly with the TG weight losses, indicating the highly representative character of Py–FIMS for the SOM status in the samples.

Temperature profiles of selected classes of chemical compounds were computed from Py–FIMS data of SOM for the first time, to the best of our knowledge. The curves of alkylaromatics and lignin dimers point to considerable thermal stabilization of these compounds even after 20 years of SOM maturation. This can be due to the three-dimensional combination of the molecular building blocks, as well as to organo–mineral interactions. Hence, the investigation of the energetic status of these bondings appears to be an interesting aspect of forthcoming thermal analytical studies of SOM.

ACKNOWLEDGEMENTS

This study was financially supported by the Deutsche Forschungsgemeinschaft, Bonn-Bad Godesberg (projects Schu 416/15-1 and Schu 416/12-3). The authors are very grateful to Professor em. Dr. G. Reuter, University of Rostock, for the generous gift of the whole soil samples. Mr. Müller, Institut Fresenius, Taunusstein, is acknowledged for this technical assistance and for recording the FI mass spectra. The authors are indebted to Mrs. Hopp and Mr. Wegener, University of Rostock, for their help with the particle-size fractionations and chemical analyses. We thank Mr. Fangmann, University of Osnabrück, for preparing Figs. 1–3.

REFERENCES

1 M. Schnitzer and I. Hoffman, Geochim. Cosmochim. Acta, 29 (1965) 859.
2 M. Schnitzer and I. Hoffman, Soil Sci. Soc. Am., Proc., 28 (1964) 520.
3 C. Anghern-Bettinazzi, P. Lüscher and J. Hertz, Z. Pflanzenernähr. Bodenkd., 151 (1988) 177.
4 J. Bachmann and H. Zhang, Z. Pflanzenernähr. Bodenkd., 154 (1991) 47.

5 H. Peschke, S. Kretschmann and S. Zeise, Arch. Acker-Pflanzenbau Bodenkd., 35 (1991) 49.
6 M. Vandenbroucke, R. Pelet and Y. Debyser, Geochemistry of humic substances in marine sediments, in G.R. Aiken, D.M. McKnight and R.L. Wershaw (Eds.), Humic substances in Soil Sediment and Water. Geochemistry, Isolation and Characterization, Wiley, New York, 1986, pp. 258–261.
7 R. Hempfling and H.-R. Schulten, Z. Pflanzenernähr. Bodenkd., 154 (1991) 425.
8 H.-R. Schulten and P. Leinweber, Biol. Fertil. Soils, 12 (1991) 81.
9 H.-R. Schulten, R. Hempfling, K. Haider, F. F. Gröblinghoff, H.-D. Lüdemann and R. Fründ, Z. Pflanzenernähr. Bodenkd., 153 (1990) 97.
10 H.-R. Schulten and R. Hempfling, Plant Soil, 142 (1992) 259.
11 R. Hempfling, H.-R. Schulten and R. Horn, J. Anal. Appl. Pyrolysis, 17 (1990) 275.
12 P. Leinweber, P. Kahle and H.-R. Schulten, Z. Pflanzenernähr. Bodenkd., 154 (1991) 169.
13 P. Leinweber, H.-R. Schulten and C. Horte, Thermochim. Acta, 194 (1992) 175.
14 G. Reuter, Arch. Acker-Pflanzenbau Bodenkd., 25 (1981) 277.
15 G. Reuter, Arch. Acker-Pflanzenbau Bodenkd., 35 (1991) 371.
16 G. Reuter, Arch. Acker-Pflanzenbau Bodenkd., 30 (1986) 273.
17 P. Leinweber and G. Reuter, Biol. Fertil. Soils, (1992), in press.
18 H.-R. Schulten, N. Simmleit and R. Müller, Anal. Chem., 59 (1987) 2903.
19 P.R. Lattimer and H.-R. Schulten, Int. J. Mass Spectrom. Ion Phys., 52 (1983) 105.
20 H.-R. Schulten and M. Schnitzer, Sci. Total. Environ., 117/118 (1992).
21 M. Schnitzer and H.-R. Schulten, Soil Sci. Soc. Am. J., in press.
22 H.-R. Schulten, J. Anal. Appl. Pyrolysis, 12 (1987) 149.
23 R.E. Grim, Clay Mineralogy, McGraw-Hill, New York, 1953.
24 S. Shoval, Thermochim. Acta, 135 (1988) 243.
25 T. Satoh, Soil Sci. Plant Nutr. (Tokyo), 30 (1984) 95.
26 P. Leinweber and G. Reuter, Mitt. Dtsch. Bodenkd. Ges., 66/II (1991) 1101.
27 B. Plage and H.-R. Schulten, Makromol. Chem., 192 (1991) 1567.
28 B. Plage and H.-R. Schulten, J. Anal. Appl. Pyrolysis, 19 (1991) 285.
29 H.-R. Schulten, P. Leinweber and G. Reuter, Biol. Fertil. Soils, submitted for publication.
30 H.-R. Schulten, B. Plage and M. Schnitzer, Naturwissenschaften, 78 (1991) 311.